Progress In Electromagnetics Research M, Vol. 50, 65–73, 2016

Design of a Dual-Band MIMO Dielectric Resonator Antenna with Pattern Diversity for WiMAX and WLAN applications

Aftab A. Khan[1, *], Mohd. Haizal Jamaluddin[2], Jamal Nair[1, 2], Rizwan Khan[1], Sajid Aqeel[1], Jawad Saleem[1], and Owais[1]

Abstract—In this paper, a dual-band multiple-input multiple-output dielectric resonator antenna (DRA) with pattern diversity is presented. L-shape of the DRA produces patterns diversity at the lower band whereas, at the upper band, it is caused by exciting TE^x_{121}/TE^y_{211} mode in the DRA. Two copper strips are pasted at the corner of the dielectric radiator to improve matching at both the bands. A cylindrical air-gap introduced in the radiator improves isolation up to 25 dB and 20 dB at lower and upper frequency bands, respectively. The MIMO system possesses pattern diversity and isolation without applying any special decoupling technique. The design covers the WiMAX and WLAN bands at 3.6 and 5.2 GHz, respectively. Simulated and measured reflection coefficients, envelope correlation, diversity gain and mean effective gain, are in good agreement.

1. INTRODUCTION

Wireless communication systems require much higher data rates for current and future communication applications. Due to the upper limit on data rate for single-input single-output (SISO) link, the only way to increase the capacity is by increasing the transmitting power or the bandwidth [1]. However, due to the limitation, bandwidth and transmitted power cannot be increased beyond a certain limit. The solution to this problem is to use more than one antenna in order to create diversity for MIMO applications [2].

Antenna diversity is useful to reduce outages, counter multipath and to improve reliability/quality of the communication link. Three types of diversity schemes can be used such as spatial diversity, polarization diversity and beam pattern diversity. In the case of spatial diversity, multiple antenna elements are spaced apart whereas, in polarization diversity, antennas are oriented orthogonally to each other. In the case of pattern diversity, co-located antennas have radiation patterns, oriented in different directions. Numerous research works can be found in literature regarding pattern diversity achievement using multiple antenna elements; however, achieving pattern diversity using a single radiator is challenging [3, 4]. In the proposed work, pattern diversity has been achieved by using an L-shaped Dielectric resonator antenna (DRA) with modes excited in the single element L-shaped dielectric resonator antenna.

DRA, due to its attractive features, has gained overwhelming importance for MIMO applications. DRA is a three-dimensional structure bearing features such as high bandwidth, high radiation efficiency, ease of excitation, high gain and negligible losses at high frequencies [5, 6]. Furthermore, infinitely many modes can be excited in a single dielectric resonator (DR). Each mode corresponds to a different resonant frequency.

Received 1 July 2016, Accepted 4 September 2016, Scheduled 20 September 2016

* Corresponding author: Aftab A. Khan (aftabjadoon@ciit.net.pk).

[1] COMSATS Institute of Information Technology, Abbottabad, Pakistan. [2] Faculty of Electrical Engineering, Wireless Communication Centre (WCC), UniversitiTeknologi Malaysia, Johor Bahru, Malaysia.

Few works have been found in literature regarding pattern diversity for MIMO applications. In [7], the authors proposed a multi-band MIMO with pattern diversity at DVB-H, WiFi and WLAN bands. In this work the authors achieved very good results in terms of diversity patterns, but two DR elements have been used, and isolation at all bands is poor. The ground size is large as well. The authors in [8] proposed an omnidirectional circularly polarized DRA with top loaded alford loop for pattern diversity. The design has been comprehensively analyzed for WLAN band with good simulated and measured results.

In the proposed work, a dual-band MIMO DRA is designed and fabricated for pattern diversity applications. It covers entire WiMAX and WLAN bands achieved through an L-shaped DRA excited by symmetrical feeding. The rest of the paper is organized as follows.

Section 2 describes antenna design and analysis. Parametric analysis based on simulated results is discussed in Section 3. Section 4 presents measured results and discussion while Section 5 concludes this paper.

2. ANTENNA DESIGN AND ANALYSIS

The proposed design is composed of an L-shaped DRA of permittivity ε_r and dimensions a, b and d, as shown in Figure 1. It is placed on an FR4 substrate of dimension $L \times L \times h$ and permittivity ε_s. The ground plane is etched on top of the substrate of the same dimensions. A cylindrical air-gap of radius r and depth d is introduced in the DR in order to improve isolation at both the bands. Two copper strips, each with dimension $l_s \times w_s$, are attached at the corner of the DRA to achieve impedance matching at both the bands. As the mode excited at 3.6 GHz, which is TE_{111}, is dominant mode, having radiation pattern in broadside direction [9], in order to achieve pattern diversity, DR is cut into an L-shape which changes radiation direction at this band. Pattern diversity at 5.2 GHz is achieved by making use of higher order TE^x_{121}/TE^y_{211} mode in x- and y-direction. This higher order mode does not have pattern in the broadside direction, hence gives pattern diversity at the upper band [10]. By slightly increasing the aspect ratio of the DR, higher order TE_{113} mode can also be excited. Two microstrip feed lines, each of dimension $m_L \times m_W$, are placed at the bottom of the substrate in order to excite the DRA through two slots of dimensions $s_w \times w$. The values of all variables shown in Figures 1(a) and 1(b) are listed in Table 2.

Table 1. Dimensions of the proposed design.

Variable	Val (mm)	Variable	Val(mm)	Variable	Val(mm)	Variable	Val(mm)
a	31.4	b	31.4	d	18.5	w	10.5
w_s	8	l_s	16.1	r	1.5	L	60
h	1.6	m_L	28.9	m_W	3	s_W	2.6
ϵ_r	10	ϵ_s	4.6				

Resonant frequency of the cubic structures can be calculated using dielectric waveguide model (DWM) [9]. As no such calculation, thus far, has been done on that of the proposed structure, initial calculation has been performed on rectangular structure of dimensions $a \times b \times d$ using [9], and it is found to be 3.1 and 5.05 GHz, respectively. The difference is due to the cut in L-shape and cylindrical air-gap in the DRA.

3. PARAMETRIC STUDY AND DISCUSSION

The proposed design is simulated in Ansoft HFSS v 15 [11]. The most important parameters to achieve high isolation and impedance matching are cylindrical air-gap depth and copper strips at the corner of the DRA. Therefore, in this work, parametric studies have been performed on these two parameters.

Figure 2 shows the simulated S_{21} for different values of cylindrical air-gap depth d. As d increases, value of S_{21} is decreased. In order to achieve optimal results, d is chosen to be 18.5 mm. The process of isolation can also be verified by analyzing electric field effects at 3.6 GHz through both the ports in

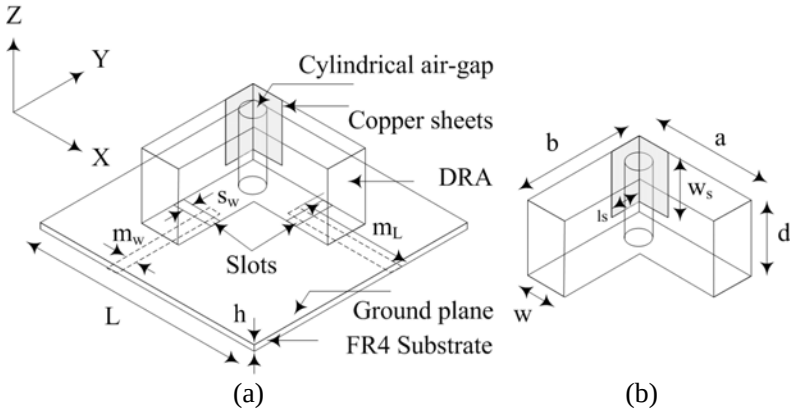

Figure 1. Perspective view of the design, (a) complete design, (b) only DR with metallic stripes at the corner.

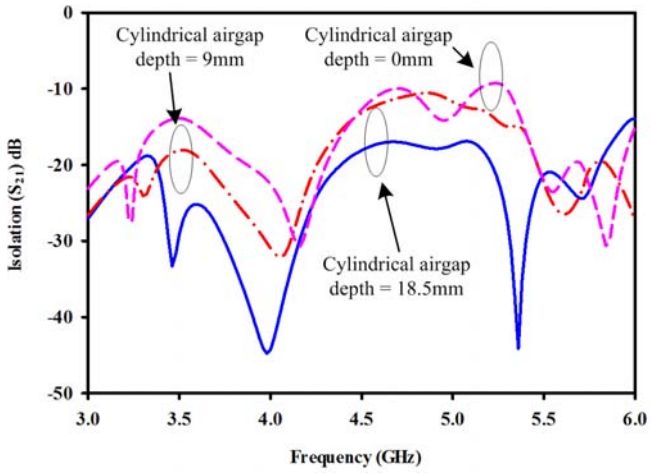

Figure 2. Isolation (S_{21}) for different values of cylindrical air-gap.

the dielectric resonator with and without cylindrical air-gap as shown in Figure 3. Figure 3(a) shows how the field intersects through both the ports (indicated by red circle) which causes poor isolation at both the bands. When the cylindrical air-gap is introduced, field through both the ports is affected at the interface of air-gap, due to the difference of permittivities, as shown in Figure 3(b). This results in improvement in isolation. Figure 3(c) shows a similar effect in the presence of copper strips at the corner of the radiator.

Figure 4 shows the effect of various copper strip heights L_s on S_{11}. Due to the symmetry of the design, the effect is the same on S_{11} and S_{22}; therefore, only S_{11} is presented in the figure. It is clearly revealed that when heights of both the strips increase simultaneously, impedance matching improves, and optimal value is achieved for 18.5 mm.

4. SIMULATED AND MEASURED ANTENNA PERFORMANCES

The prototype of the MIMO dual-band antenna is fabricated as shown in Figure 5(a) (3D-view) and 5b (bottom view). The DR is made of Eccostock HK-10 from Emerson and Cuming® of permittivity 10 and tangent loss 0.002. The DRA is excited through slots feeding by two microstrip feed lines etched on the opposite side of the substrate. The measured impedance bandwidth covers both WiMAX and WLAN bands comfortably. Figure 6 shows the comparison of simulated and measured S-parameters,

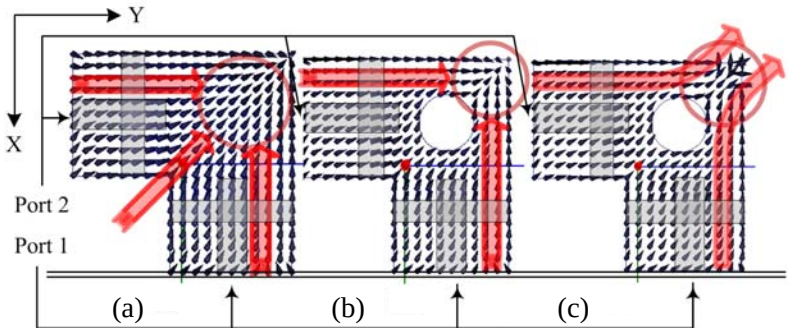

Figure 3. Electric field effect in the radiator, (a) without air-gap, (b) with air-gap, (c) with air-gap and copper strips at the corner.

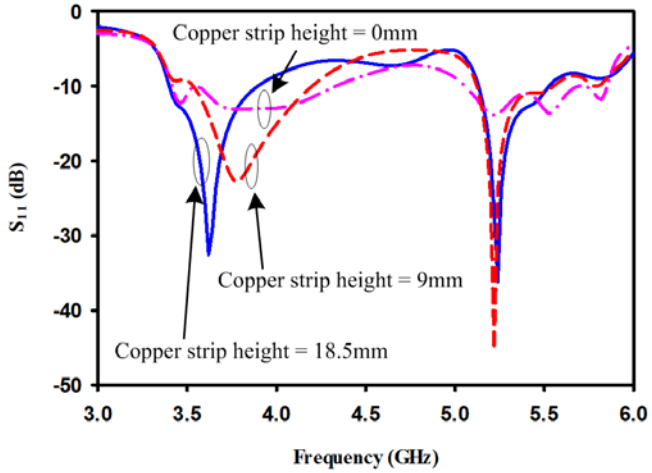

Figure 4. Effect of various copper sheet heights on S_{11}.

and the corresponding impedance bandwidths are listed in Table 2. The difference in simulated and measured results is due to the fabrication tolerances.

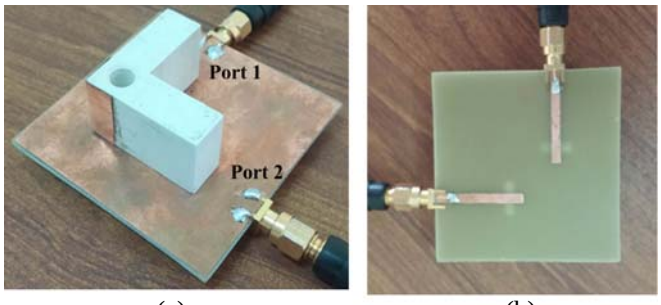

Figure 5. Prototype of the fabricated antenna, (a) 3D-view, (b) bottom view.

The electric field distribution for TE^x_{111}/TE^y_{111} and TE^x_{211}/TE^y_{121} modes excited at 3.6 and 5.2 GHz are shown in Figures 7(a) and (b), respectively.

The total efficiency ($\mu_{i,total}$) for port 1 and port 2 has been calculated using Equations (1) and (2), respectively [12], where $\mu_{i,rad}$ is the radiation efficiency for port i. Radiation efficiency is always greater

Table 2. Simulated and measured impedance bandwidth.

Bandwidth	Lower Band (GHZ)		Upper Band (GHz)	
	Port 1	Port 2	Port 1	Port 2
Simulated	3.40–3.90	3.40–3.90	5.12–5.54	5.12–5.54
Measured	3.42–3.80	3.37–3.78	4.97–5.50	4.70–5.35

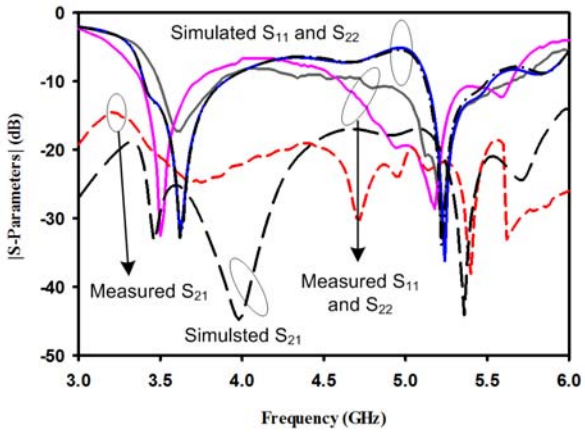

Figure 6. Measured and simulated S-parameters.

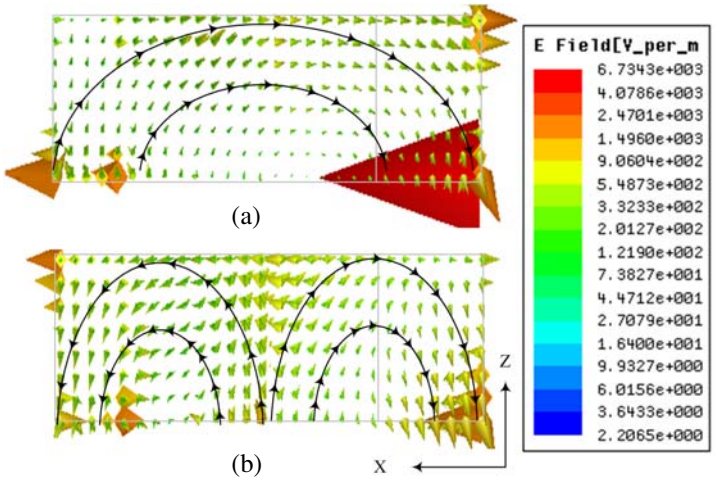

Figure 7. Electric field patterns, (a) TE_{111}, (b) TE_{211}.

than the total efficiency as it does not take into account surface current losses. The total efficiency for both the ports at 3.6 GHZ is 92% and at 5.2 GHZ is 91 %. Similarly, due to the symmetry of the design, gains for both ports at 3.6 GHz and 5.2 GHz are 5.2 and 6.38 dBi, respectively.

$$\mu_{1,total} = \mu_{1,rad}\left(1 - |S_{11}|^2 - |S_{21}|^2\right) \quad (1)$$

$$\mu_{2,total} = \mu_{2,rad}\left(1 - |S_{22}|^2 - |S_{12}|^2\right) \quad (2)$$

Figures 8 and 9 show simulated and measured co- and cross radiation patterns in E- and H-planes at 3.6 GHz and 5.2 GHz, respectively. In both the figures, the maximum gains for the two ports at 3.6 GHz are toward -60^0 and $+60^0$. Similarly at 5.6 GHz, direction of the beam is towards -55^0 and $+55^0$. In Figures 8 and 9, cross-polarization (X-polarization) is reasonably lower than co-polarization,

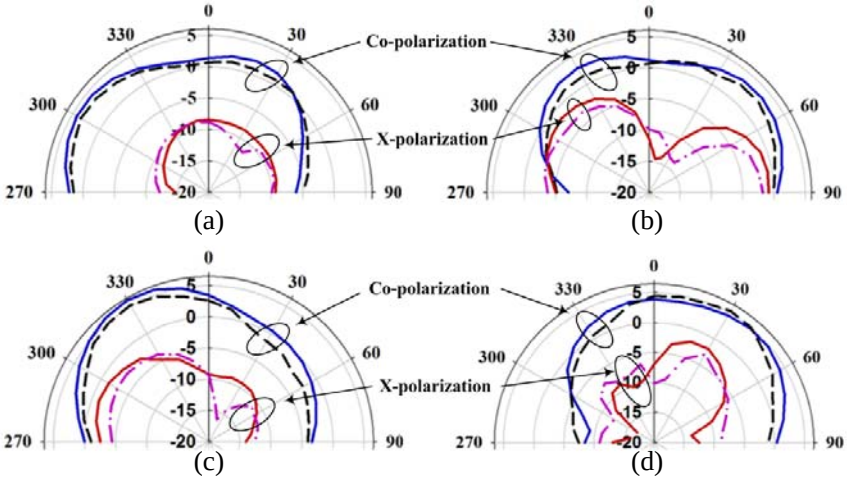

Figure 8. Simulated and measured radiation pattern (E-planes). (a) Port1 3.6 GHz. (b) Port2 3.6 GHz. (c) Port1 5.2 GHz. (d) Port2 5.2 GHz. (solid lines — simulated, dash lines — measured).

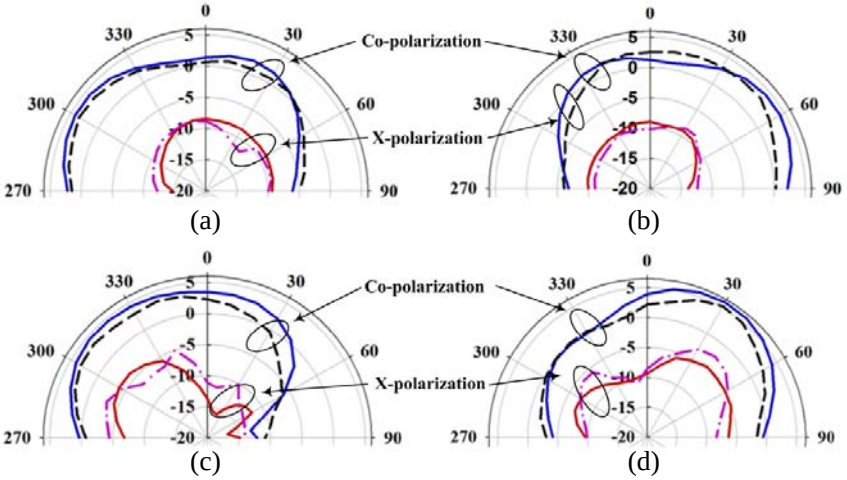

Figure 9. Simulated and measured radiation pattern (H-planes). (a) Port1 3.6 GHz. (b) Port2 3.6 GHz .(c) Port1 5.2 GHz. (d) Port2 5.2 GHz. (solid lines — simulated, dash lines — measured)

still within the acceptable limit. Figure 10 shows 3-D plot both at 3.6 GHz and 5.2 GHz. Black circles indicate the direction of the maximum beam.

Envelope correlation coefficient (ECC) is used to find the correlation between signals received by the antenna. In this paper, ECC has been calculated using Equation (3) given in [12]. Figure 11 shows simulated and measured ECC using Equation (3). It is clear from the figure that measured ECC at both the bands is below 0.01, which shows good MIMO performance.

$$\rho = \frac{|S_{11}^* S_{12} + S_{21}^* S22|^2}{(1 - |S_{11}|^2 - |S_{21}|^2)(1 - |S_{22}|^2 - |S_{12}|^2)} \tag{3}$$

The second important MIMO parameter is the diversity gain (DG). It is the amount of improvements obtained from multiple to single antenna systems. The diversity gain can be calculated using DG equation, given in [13]. The value of simulated and measured DG shown in figure 12 at both the bands is almost 10 dB, which ensures good MIMO performance.

The last MIMO parameter to be analyzed in this work is the mean effective gain (MEG). It is the power received by the diversity antenna relative to the power received by an isotropic antenna. MEG

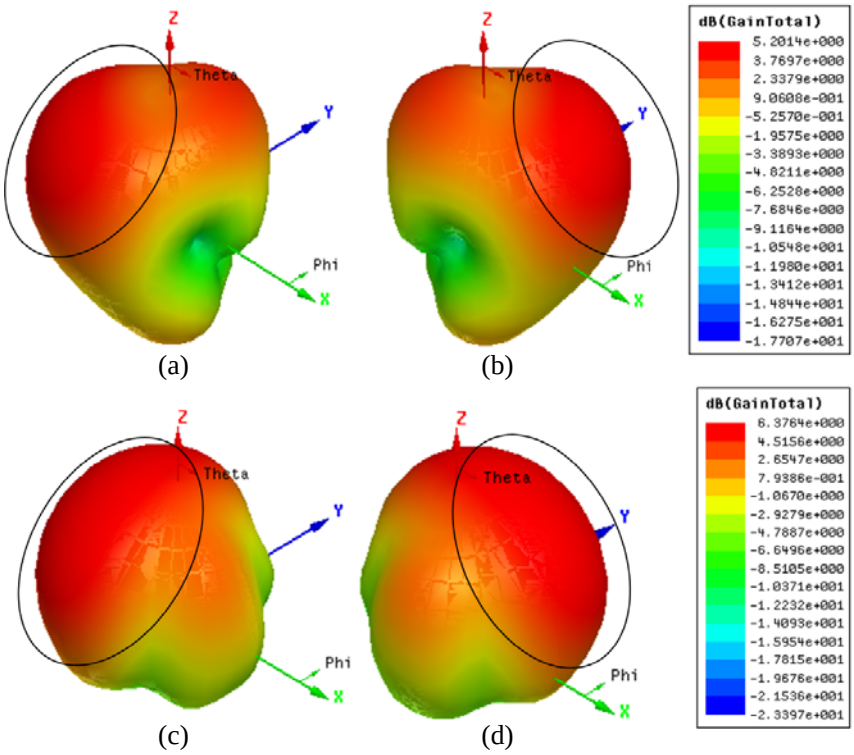

Figure 10. 3-D radiation pattern at 3.6 GHz and 5.2 GHz for the two inputs. (a) Port1 3.6 GHz. (b) Port2 3.6 GHz. (c) Port1 5.2 GHz. (d) Port2 5.2 GHz.

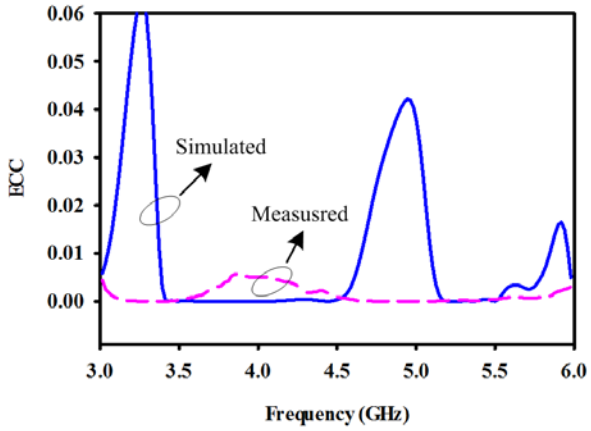

Figure 11. Simulated and measured envelope correlation coefficient (ECC).

can be calculated using Equation (4). For a similar power level at each branch, the power ratio k must be less than 3 dB [14].

$$MEG_i = 0.5\mu_{i,rad} = 0.5 \left(1 - \sum_{j=1}^{M} |S_{ij}|\right) \tag{4}$$

where M is the number of antennas and $k = |MEG1 - MEG2|$ in dB. Figure 13 shows the measured MEGs of the proposed antenna. It clearly indicates that the power ratio k is below 3 dB, as required.

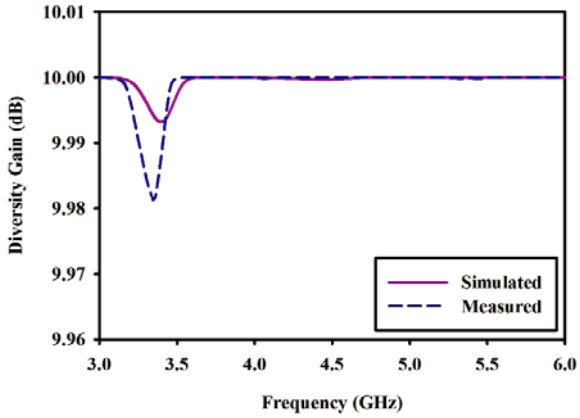

Figure 12. Simulated and measured diversity gain (DG).

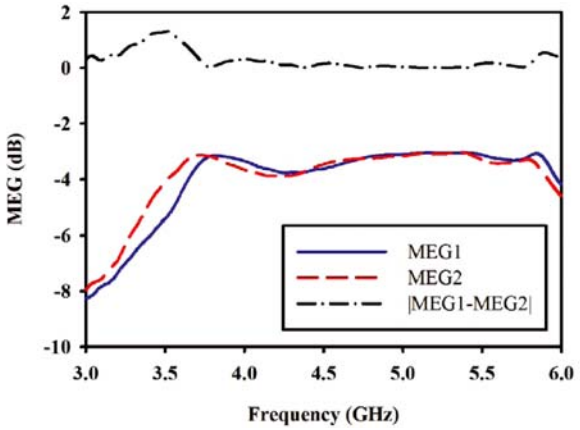

Figure 13. Measured mean effective gain (MEG) and power ratio, k.

5. CONCLUSION

In this work, a dual-band MIMO DRA with pattern diversity capability for WiMAX/WLAN bands is proposed and investigated. The pattern diversity is achieved using an L-shaped DRA by exciting TE^x_{111}/TE^y_{111} modes at 3.6 GHz, and using TE^x_{121}/TE^y_{211} modes excited at 5.2 GHz bands, respectively. Almost 25 dB and 20 dB isolations have been achieved by making use the cylindrical air-gap in the DRA. Total efficiency achieved at both the bands is better than 91%. Simulated and measured S-parameters are in good agreement. Results of measured ECC, DG and MEG ensure good MIMO performance. Similarly, gain at lower band is 5.2 dBi and at upper band is 6.38 dBi. The presented results indicate that the proposed antenna is suitable for pattern diversity applications for WiMAX/WLAN bands.

ACKNOWLEDGMENT

The authors would like to thank the Ministry of Education (MOE) and UTM GUP (votes 05H62) and Ministry of Science Technology and Innovation (MOSTI) (vote 4S056) for sponsoring this work.

REFERENCES

1. Paulraj, A. J., D. A. Gore, R. U. Nabar, and H. Bolcskei, "An overview of MIMO communications — A key to gigabit wireless," *Proceedings of the IEEE*, Vol. 2, 198–218, 2004.

2. Addaci, R., D. Seetharamdoo, M. H. Rabah, and M. Berbineau, "Multi-band multi-antenna system for diversity and/or MIMO applications," *International Journal of Research in Wireless Systems*, Vol. 2, 17, 2013.
3. Malik, J., D. Nagpal, and M. V. Kartikeyan, "MIMO antenna with omnidirectional pattern diversity," *Electronics Letters*, Vol. 2, No. 52, 102-4, 2016.
4. Malik, J., A. Patnaik, and M. V. Kartikeyan, "Capacity estimation of a comapct pattern diversity MIMO antenna," *International Conference on Microwave, Optical and Communication Engineering (ICMOCE)*, 25–28, 2015.
5. Petosa, A., *Dielectric Resonator Antenna Handbook*, Artech House Publishers, 2007.
6. Khalily M., M. R. Kamarudin, and M. H. Jamaluddin, "A novel square dielectric resonator antenna with two unequal inclined slits for wideband circular polarization," *IEEE Antenna and Wireless Propagation Letters*, Vol. 12, 1256–1259, 2013.
7. Huitema, L., M. Koubeissi, E. Arnaud, C. Decroze, and T. Monediere, "Compact and multiband dielectric resonator antenna with pattern diversity for multistandard mobile handheld devices," *IEEE Transaction on Antennas and Propagation*, Vol. 59, 4201–4208, 2011.
8. Li,W. W. and K. W. Leung, "Omnidirectional circularly polarized dielectric resonator antenna with top-loaded alford loop for pattern diversity design," *IEEE Transaction on Antennas and Propagation*, Vol. 8, 4246–4256, 2013.
9. Fang, X. S. and K. W. Leung, "Designs of single-, dual-, wide-band rectangular dielectric resonator antennas," *IEEE Transaction on Antennas and Propagation*, Vol. 59, 2409–2414, 2011.
10. Raggad, H., M. Latrach, A. Gharsallah, and T. A. Razban, "Compact dual band dielectric resonator antenna for wireless applications," arXiv preprint arXiv, 1306.1335, 2013.
11. HFSS: ANSYS based on 3-D full-wave electromagnetic fields technique, 2014, Available: http://www.ansys.com/Products.
12. Nasir, J., M. H. Jamaluddin, M. Khalily, M. R. Kamarudin, I. Ullah, and R. Selvaraju, "A reduced size dual port MIMO DRA with high isolation for 4G applications," *International Journal of RF and Microwave Computer Aided Engineering*, Vol. 25, 495–501, 2015.
13. Roslan, S. F., M. R. Kamarudin, M. Khalily, and M. H. Jamaluddin, "An MIMO rectangular dielectric resonator antenna for 4G applications," *IEEE antennas and wireless propagation letters*, Vol. 13, 321–324, 2014.
14. Zou. L., D. Abbott, and C. Fumeaux, "Omnidirectional cylindrical dielectric resonator antenna with dual polarization," *IEEE Antennas Wireless Propagation Letters*, Vol. 11, 515–518, 2012.